Relaxation phenomena of image sensors made from *a*-Si:H

M. Hoheisel, N. Brutscher, and H. Wieczorek[a)]
Siemens AG, Corporate Research and Development, Otto-Hahn-Ring 6, D-8000 München 83, Federal Republic of Germany

(Received 17 February 1989; accepted for publication 6 July 1989)

Image sensors made from amorphous silicon (*a*-Si:H) are under development. Their elements consist of back-to-back Schottky diodes. For practical operation, long-term stability is of great importance. We investigated dark conductivity and photoconductivity, capacitance-voltage characteristics, and response behavior after switching off illumination. Even after light soaking for many hours, no change in photocurrent occurred, whereas dark current, capacitance, and response time increased. These changes are metastable and can be reversed by annealing above 200 °C. Contrary to the Staebler–Wronski effect, [Appl. Phys. Lett. **31**, 292 (1977)], the dark-current increase disappears at room temperature after several hours. We investigated the time dependence of this relaxation and calculated the energetic depth of the states involved. The contact between *a*-Si:H and indium-tin-oxide is described as a Schottky–Bardeen-metal-insulator-semiconductor junction. Its properties are strongly dependent on interface states, in particular on the position of the neutrality energy of the interface states with respect to the Fermi energy. We show that besides the well-known Staebler–Wronski effect, a new degradation process is observed. We suggest a model where holes are trapped in interface states about 1.0–1.4 eV above the valence band. Their thermal emission governs the relaxation behavior of the dark current.

I. INTRODUCTION

Easier reading of documents for communication and office automation calls for large-area scanners that can read A4-size documents without optical reduction. Therefore, large-area thin-film photoconductors are required that can be fabricated at least 21 cm wide at low cost. The most promising way to implement such a device is an arrangement of amorphous silicon (*a*-Si:H)sandwiched between two electrodes forming Schottky-type contacts. A review of such image sensors has been given by Kempter.[1]

Our sensors are built in the sequence Cr/*a*-Si:H/ITO. Their elements meet the most important requirements for image sensors: high photocurrent, low dark current, fast response behavior, and long-term stability.[2] In this paper we present an investigation of the stability of the sensor based on the physics of the junction involved.

As the elements are reverse biased (ITO negative) during operation, the properties of the *a*-Si:H/ITO junction are crucial for the performance of the sensing element. To obtain a low dark current and an enhanced chemical stability, an intermediate oxide layer is introduced between *a*-Si:H and indium-tin oxide (ITO). Thus, strictly speaking, the contact is a metal-insulator-semiconductor (MIS) junction. On the one hand, this junction can be described by the Schottky theory, but on the other hand, interface states play an important role in the performance of the junction; so the Bardeen theory should also be applied. We will therefore call it a Schottky–Bardeen-MIS junction (SBMIS junction).

II. THEORY OF THE SCHOTTKY–BAROEEN-MIS JUNCTION

To explain a SBMIS junction, we start from an ideal metal-semiconductor contact. The Schottky theory[3–5] predicts the barrier height Φ_B of the Schottky contact from the work function of the metal Φ_M and the electron affinity of the semiconductor χ:

$$e\Phi_B = e\Phi_M - e\chi. \tag{1}$$

The difference between the barrier height and the activation energy $E_c - E_F$ in the bulk of the semiconductor leads to a charge transfer from the semiconductor to the metal, resulting in a positive space charge and a band bending with a diffusion voltage V_D:

$$eV_D = e\Phi_B - (E_c - E_F). \tag{2}$$

ITO shows an almost metal-type conductivity in excess of $10^4\ (\Omega\ \mathrm{cm})^{-1}$. Although it is a highly doped semiconductor, it can be treated as a metal for our investigations.

It is well known that interface states play an important role in the vicinity of the metal-semiconductor contact. This is explained by the Bardeen theory.[6] It leads to an expression for the barrier height that depends on the energy gap E_G of the semiconductor, not on the work function of the metal used:

$$e\Phi_B = E_G - e\Phi_0. \tag{3}$$

$e\Phi_0$ denotes the energy difference between the neutrality level of the interface states and the Fermi level. Equation (3) can be understood as follows: The interface states are filled up to the Fermi level E_F. Suppose the neutrality level E_n of these states is E_v and thus lower than E_F by an energy $e\Phi_0$. The interface states are then negatively charged. An equal amount of charge of the opposite sign forms the space-

[a)] Permanent address: Philips GmbH, Research Laboratories, Weisshausstrasse, D-5100 Aachen, FRG.

 0021-8979/89/214466-08$02.40

charge region inside the semiconductor. With a high interface-state density and a low density of states inside the semiconductor, this leads to a pinning of the Fermi energy at the interface.

The theories discussed above outline the two limiting cases. The barrier height of a real diode must be described by a combination of both the Schottky and the Bardeen barriers.

Introduction of an intermediate oxide layer leads to an MIS junction. Without a space charge inside the insulator and without interface states, the electric field will be constant throughout the insulator and at the interface. This leads to a voltage drop ΔU across the insulator which decreases the barrier height:

$$e\Phi_B = e\Phi_M - e\chi - e\Delta U. \tag{4}$$

In an SBMIS, the interface states result in a partial pinning of the Fermi energy at the interface, reducing the influence of the metal's work function. The electric field at the interface has a kink due to the interface charge. A change of the charge dQ per unit area A causes an equivalent modification of the electric field dU/d_i where ϵ_i is the dielectric constant of the insulator and d_i its thickness:

$$dU = +\frac{d_i}{\epsilon\,\epsilon_i A}\,dQ. \tag{5}$$

The plus sign applies to the voltage drop as depicted in Fig. 1(a); i.e., a negative charge at the interface leads to a lower voltage drop ΔU and thus to a higher barrier.

We can now discuss the different changes that can occur at an SBMIS junction during degradation. Two different mechanisms will be considered. Either new states are created by degradation or existing states become negatively or positively charged.

Let us discuss the first case. New states can be created either in the bulk of the semiconductor or at the interface. What will happen to the barrier? When the density of states in the bulk is increased in the energy interval between E_F and $e\Phi_B$ [i.e., the shaded area marked as positive space charge in Fig. 1 (a)], it is obvious that these states have to be recharged positively and the band-bending profile will change accordingly. Hence the barrier will become narrower. If interface states are increased, their influence upon the barrier depends on the position of their neutrality energy. For simplicity we assume that the newly created states are of the same type as the existing ones. Suppose their neutrality level E_n is lower than the Fermi level E_F [Fig. 1(a)], then the newly created states have to be filled with electrons, thus increasing the negative interface charge. This diminishes the voltage drop ΔU along the insulator according to Eq. (5). As Eq. (4) shows, the barrier $e\Phi_B$ will increase. The opposite will happen when states with $E_n > E_F$ are created [Fig. 1(b)]. These states have to be filled with holes, thus increasing the positive interface charge. Hence ΔU will increase and Φ_B will decrease.

We will now discuss the case of recharging existing states. When electrons are trapped in bulk states, they compensate the positive space charge. This leads to a lower band bending and thus to a diminished barrier height. Correspondingly, the capture of holes leads to a stronger band bending and to an increased barrier height. If trapped electrons are localized in interface states, this negative interface charge will increase the barrier [Eqs. (4) and (5)], whereas hole capture at the interface decreases it. A summary of all cases is given in Table I.

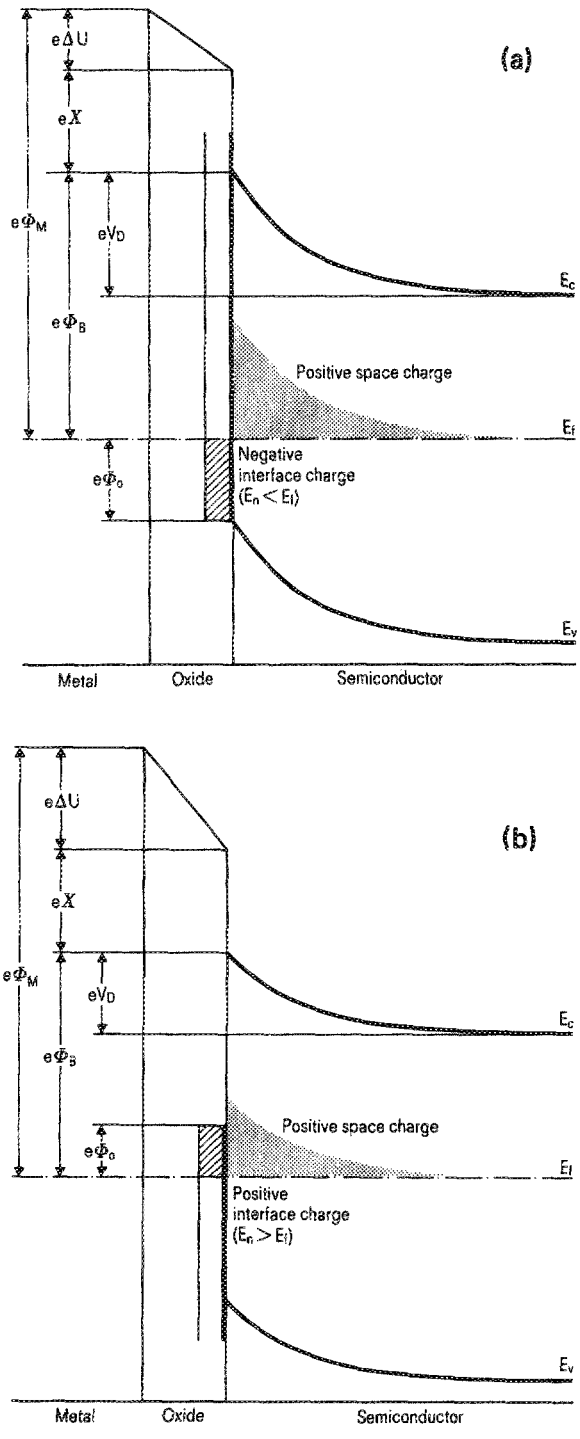

FIG. 1. Band diagram of a Schottky–Bardeen-MIS junction. The barrier height amounts to $e\Phi_B = e\Phi_M - e\chi - e\Delta U$. (a) Interface states with a neutrality energy below E_F are negatively charged; (b) those with a neutrality energy above E_F are positively charged.

III. EXPERIMENT

The samples were produced on glass substrates, as can be seen from Fig. 2(a). The bottom electrode consisting of

TABLE I. Influences upon the barrier height.

States are	Located	The barrier becomes
created	in the bulk	narrower
created	at the interface ($E_n < E_F$)	higher
created	at the interface ($E_n > E_F$)	lower
negatively charged	in the bulk	lower
positively charged	in the bulk	higher
negatively charged	at the interface	higher
positively charged	at the interface	lower

sputtered chromium was followed by an undoped a-Si:H layer, which was deposited by plasma-enhanced CVD at 220 °C and with about 1-μm thickness. Its surface was treated in an oxygen plasma to develop an oxide layer. The thickness of the oxide can be determined from the cross-sectional TEM image [Fig. 2(b)] to be about 3 nm. Then a 100-nm-thick ITO film was evaporated by means of an electron gun as a transparent upper electrode. Additional gold strip lines were used to form a low-resistive interconnection between the sensing elements and the readout circuit. Details have been described elsewhere.[7]

The dark conductivity of the a-Si:H material was measured in a gap-cell geometry in order to determine the position of the Fermi energy. The samples were n-type, and the Fermi level was typically about 0.8 eV below E_c. The barrier height of the SBMIS junctions was determined from temperature-dependent I-V characteristics. It amounted to 0.86 eV.[8] The Schottky barrier at the bottom of the samples between chromium and a-Si:H is rather low and has little influence on the performance of the device. Therefore, an n^+ layer is not necessary.

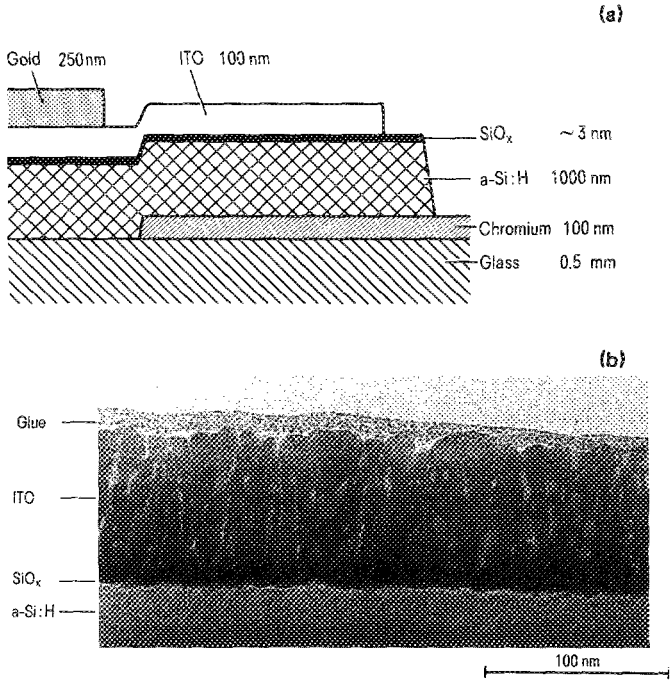

FIG. 2. (a) Schematic cross section through a sample. The deposition sequence of a typical element is glass/chromium/a-Si:H/oxide/ITO. An additional gold layer is supplied for low-resistive wiring. (b) Shows a TEM image of the oxide layer between a-Si:H and ITO (glue is necessary for preparing the TEM cross section).

From every sample we measured current-voltage characteristics in the dark and under illumination. The latter was usually 10^{14} photons/cm^2 s of green light (550 nm). Photocurrent transients were measured by switching off steady-state illumination by a Bragg cell. The current was fed through a fast current-voltage converter into a waveform recorder. The decay of the current could thus be monitored from 1 μs to 1 s after switching off the light.[9] To determine the junction capacitance, a quasistatic capacitance-voltage meter (Keithley model 595) was used. It superimposes a voltage step on a fixed bias and integrates the charge during a delay time t_d ranging from 70 ms to 200 s. An internal leakage-current correction takes care of a constant-current contribution to the integrated charge and substracts it automatically.[10]

The capacitance-delay time measurement is equivalent to a conventional capacitance-frequency measurement. The total amount of charge that is thermally emitted from occupied states is integrated during the delay time. Hence the contribution of all states closer to E_c than a certain demarcation energy E_d is included. In capacitance-frequency experiments, the same states above E_d can be charged and recharged, and thus follow the applied alternating voltage. Likewise, the density of states $N(E)$ can be computed from the $C(t_d)$ data. To obtain the $N(E)$ curves shown below (Fig. 9), we used the computer program developed by Glade *et al.*[11,12]

Most of our investigations were performed under vacuum of about 1 mPa. The influence of different ambients on the degradation behavior was shown by experiments in N_2, O_2, or air under atmospheric pressure or in saturated water vapor.

IV. RESULTS

Typical current-voltage characteristics of our SBMIS junctions are shown in Fig. 3. The annealed sample (curve A) exhibits a dark-current density at reverse bias of only 5×10^{-10} A/cm^2. The photocurrent is independent of applied voltage in the negative-bias regime. This clearly shows its primary nature. Its absolute magnitude corresponds to a quantum efficiency of unity which is diminished only by reflection losses at the ITO top electrode. The oxide layer at the interface is thin enough to have no influence on the photocurrent.

Subsequently, the degradation behavior of the devices was studied. The diodes were light soaked for 12 h with 100 mW/cm^2 white light. Under open-circuit or short-circuit conditions or with a + 5-V bias applied to the samples during illumination, only slight changes were observed. Light soaking of the diodes under negative bias (− 5 V) causes the dark current at − 5 V to increase strongly (curve B). The open-circuit voltage under illumination, recognizable by the sharp dip in the logarithmic plot, decreases, as does the short-circuit current.

Resting the sample for several days (curve R3 = 3 days, curve R30 = 30 days) at room temperature leads to a recovery of the dark-current and photocurrent characteristics.

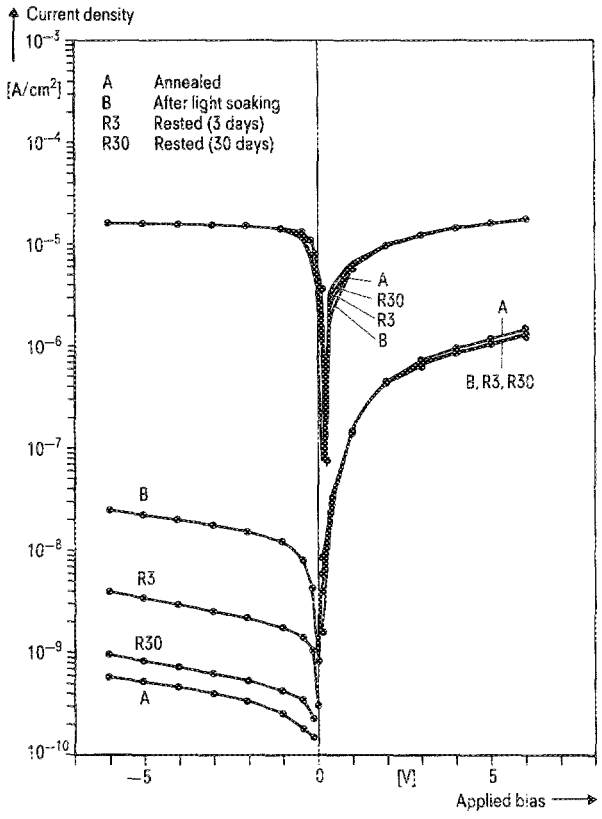

FIG. 3. Current-voltage characteristics in the dark (lower curves) and under illumination (upper curves). A = annealed state, B = after light soaking (12 h, 100 mW/cm^2), R3 = rested 3 days at room temperature, and R30 = rested 30 days at room temperature.

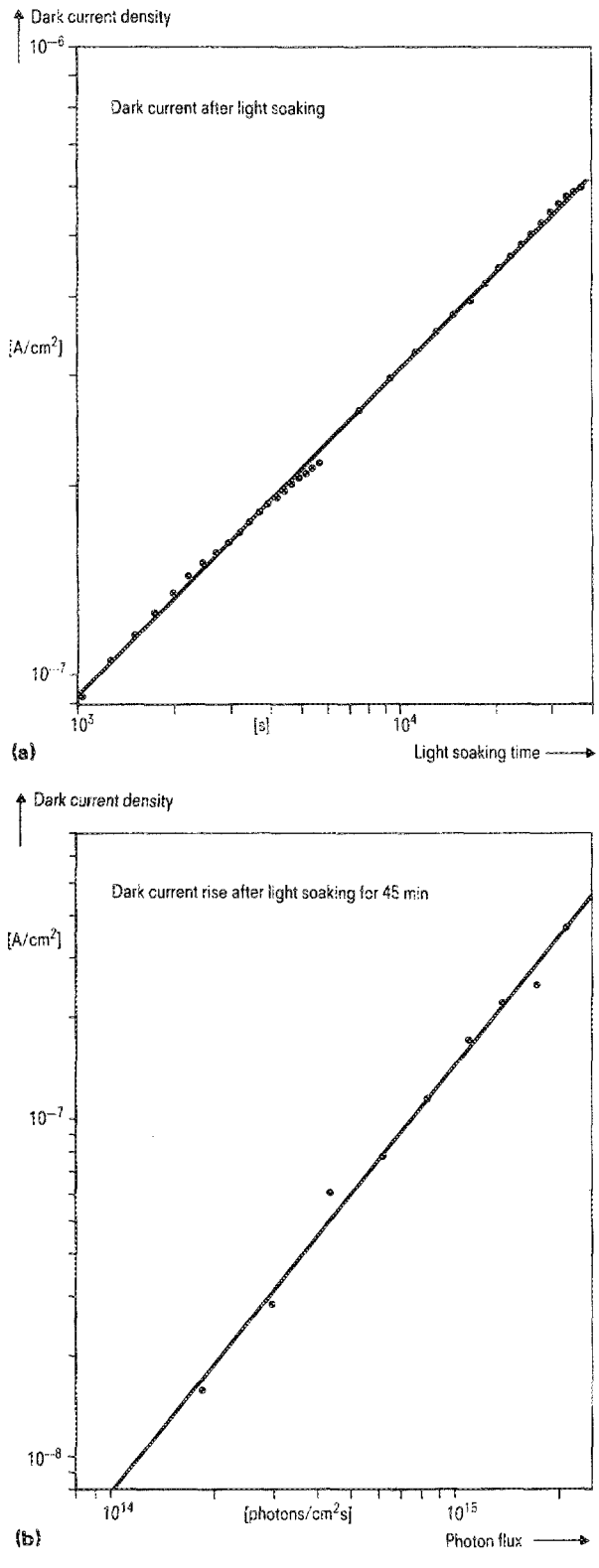

FIG. 4. Degradation behavior of the dark current I_d at -5 V bias. (a) Shows the increase of I_d with time during light soaking. (b) Shows I_d after light soaking with different photon fluxes for 45 min in each case.

The dark current approaches its low value in the annealed state (A). The open-circuit voltage and the short-circuit current also recover. When the sample is annealed again, state A is reestablished. The whole degradation cycle can be executed repeatedly.

The dark current under forward bias does not follow this trend. It decreases slightly after illumination, but does not increase during resting. This can be easily understood, as the forward current is limited by the bulk resistance of the *a*-Si:H. It is subject to the normal Staebler–Wronski degradation, which remains stable at room temperature. As the Fermi energy in the bulk material already lies near midgap, light soaking causes only a weak shift, and therefore the dark current decreases just slightly.

We studied the degradation behavior of the dark current at -5 V bias in detail. Figure 4(a) shows its increase with illumination time in a double-logarithmic plot. The light was interrupted from time to time and the dark current recorded. After a very steep rise during the first 1000 s (not shown), the current increases with the square root of time up to 10 h. In comparison, the spin density N_s rises proportionally to $t^{1/3}$.[13] However, the reverse current depends only indirectly on the spin density and is therefore not expected to exhibit the same relationship ($\sim t^{1/3}$).

Then, starting from the annealed state, we degraded the sample several times with different photon fluxes F for 45 min at each intensity [Fig. 4(b)]. This led to a very strong dependence of the dark current on F with an exponent of 1.25. For comparison, the intensity dependence of the rise of N_s has an exponent of 2/3.[13].

The relaxation of the dark current under reverse bias

(− 5 V) was investigated at different temperatures. The samples were light soaked as described above at room temperature. After switching off the illumination, they were heated quickly to the desired temperature, and the dark current was monitored over times up to 270 h. Figure 5 shows the decreasing current which reveals the features depicted in Fig. 3. The decay ranges from 1 min up to 270 h. If we assume that the basic process is a thermal emission of trapped carriers from localized states, we can convert the time scale to an energy scale by the relation

$$E = kT \ln(\nu_0 t). \tag{6}$$

For the attempt-to-escape frequency ν_0, we take a value of $10^{14}\ s^{-1}$. Hence the energies span a range of about 0.93–1.4 eV. In Fig. 6 the transients of Fig. 5 are replotted with the curves shifted relative to each other to yield a continuous trend. In the case of a diffusion-limited saturation current density j_s the barrier height can be written as

$$\Phi_B = -\frac{kT}{e}\ln\left(\frac{j_s}{eN_c\mu F}\right). \tag{7}$$

To calculate Φ_B the effective density of states in the conduction band N_c, the carrier mobility μ, and the strength of the electric field F at the interface are required. As we know neither the actual values of N_c, μ, and F nor their dependence on temperature, degradation, or relaxation, Eq. (7) only allows a general trend to be estimated. Nevertheless, the change in current indicates an increasing barrier height. From the energy interval in which the current decreases we conclude that carriers are emitted from states between 1.02–1.4 eV deep.

The photocurrent during illumination at reverse bias (− 5 V) was monitored for several hours. It showed no significant degradation and remained constant within ± 0.5% due to experimental scatter.

On the other hand, short-circuit photocurrent decay transients show significant differences between the annealed and light-soaked states. The curves recorded after switching off steady-state illumination are shown in Fig. 7(a). Electrons are trapped in localized states in the *a*-Si:H during illumination. Subsequently, these electrons are thermally emitted and extracted by the built-in field determining the

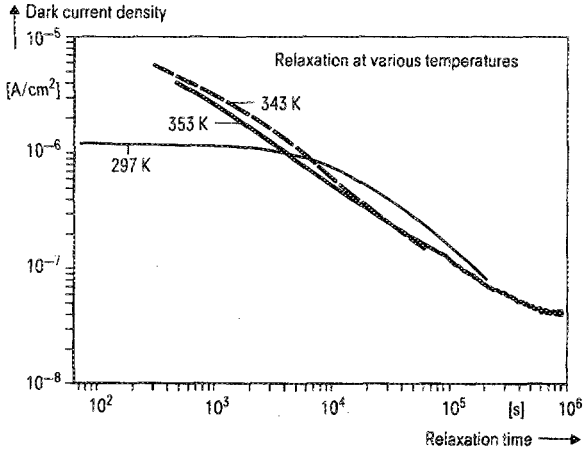

FIG. 5. Relaxational behavior of the dark current I_d at − 5 V bias at different temperatures. I_d decreases up to two orders of magnitude within 270 h.

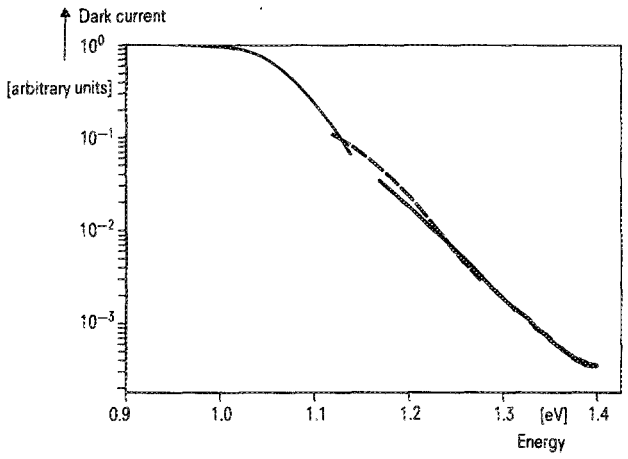

FIG. 6. Logarithm of the dark current in arbitrary units as in Fig. 5, plotted vs emission energy. The curves were shifted relative to each other, yielding the general shape of the emission process.

current decay.[14] The emission time can be converted into an energy by means of Eq. (6). The energy spectrum of the trapped charge $n(E)$ can then be calculated from the current $I(t)$ by

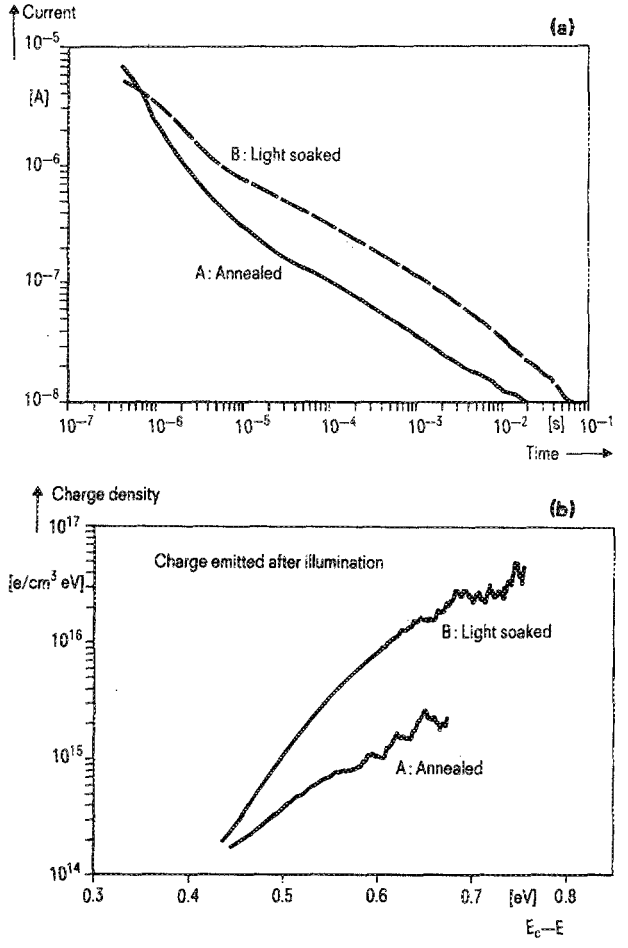

FIG. 7. (a) Photocurrent transient after switching off steady-state illumination (sample area 0.2 cm^2). (b) As the transient current is due to thermal emission of trapped electrons, the energy-resolved charge density $n(E)$ can be evaluated. Starting from the annealed sample (state A), $n(E)$ rises strongly after light soaking (state B).

$$n(E) = I(t)t/ekTV, \quad (8)$$

where V is the sample volume [Fig. 7(b)].

It should be pointed out that the measured charge density $n(E)$ is the product $N(E)f(E)$, i.e., bulk density of states $N(E)$ and occupancy of these states $f(E)$, respectively. $n(E)$ shows an increase in the energy range from 0.45 eV down to about 0.7 eV below E_c. The trend is mainly due to $f(E)$ which is dominated by a Boltzmann distribution. The shape of $N(E)$ itself cannot be resolved by this method in detail, but it reveals no distinct structure. The measured charge density rises strongly after 64 h illumination with 100 mW/cm^2 white light (state B). As $f(E)$ is expected to be the same in the light-soaked state, $N(E)$ must increase by about one order of magnitude. This can be easily understood by assuming additional dangling bonds created by the Staebler–Wronski effect.

Figure 8 shows the capacitance of the space-charge region of our SBMIS junction measured by the quasistatic method plotted versus delay time. At short times, the capacitance is equal to the geometrical capacitance of the diode. Within a certain delay time t_d, only states that are closer to E_c than the corresponding demarcation energy E_d are thermally emitted and can thus contribute to the integrated charge. In analogy to Eq. (6), E_d is given by

$$E_d = kT\ln(\nu_0 t_d). \quad (9)$$

For $t_d = 70$ ms, the shortest time interval used, and $\nu_0 = 10^{14}$ s^{-1} (Ref. 12), we obtain $E_d = 0.76$ eV. As in our samples, the position of the Fermi level, $E_c - E_F > 0.76$ eV, and the states above the demarcation energy E_d are empty and thus do not appear in the capacitance. Toward longer t_d we observe the contribution of deeper states, and the capacitance therefore increases. From this curve, the density of states $N(E)$ can be calculated.[12]

Figure 9 shows a fit to $N(E)$ around 0.8 eV. As our samples are undoped, we are restricted to a narrow energy interval. The density of states near midgap amounts to about 2×10^{16} and 3×10^{17} cm^{-3}eV^{-1} in the annealed and light-soaked samples, respectively. These results are comparable with those obtained by Glade, Beichler, and Mell[15] on undoped a-Si:H/Pt Schottky barrier diodes. The change of the capacitance spectrum after illumination, i.e., the rise from state A to state B, reflects the creation of states due to the Staebler–Wronski effect.

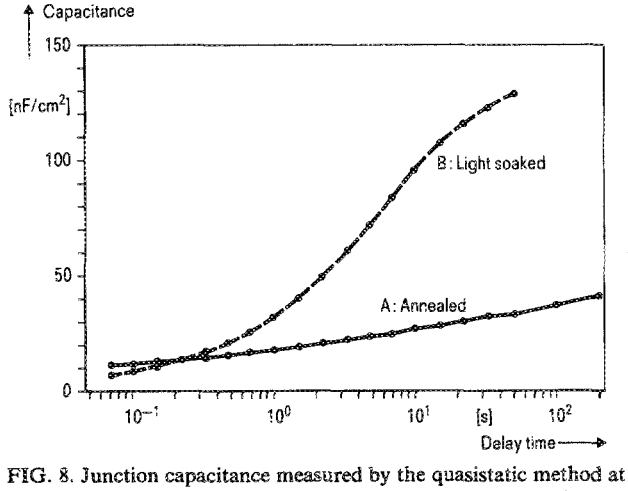

FIG. 8. Junction capacitance measured by the quasistatic method at zero bias. Delay times range from 70 ms to 200 s. Starting from the annealed sample (state A), the capacitance rises strongly after light soaking (state B).

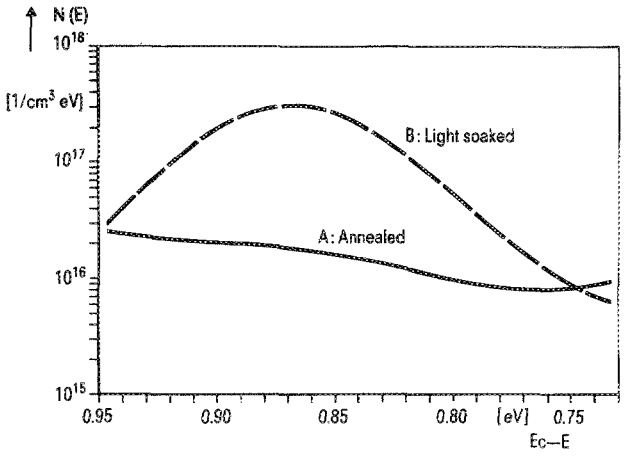

FIG. 9. Density of states $N(E)$ calculated from the junction capacitance (Fig. 8). $N(E)$ rises strongly from state A to B according to the normal Staebler–Wronski effect.

V. DISCUSSION

In our measurements we can see two different processes taking place: We observe the well-known Staebler–Wronski effect (SWE), which is metastable at room temperature. It can be annealed as usual above 200 °C. Additionally, we find a new phenomenon, a marked increase in the dark current of the SBMIS junctions after intense illumination, which is not stable at room temperature and disappears after several hours. Earlier investigations by Jousse *et al.*[16] did not concentrate on reverse-biased diodes. They found the normal SWE in the forward characteristics, but could not explain the features of the reverse current.

Let us discuss the Staebler–Wronski effect first. Illuminating an a-Si:H sample for a long time with intense white light leads to the creation of dangling bonds near midgap. This can be understood by the breaking of weak Si—Si bonds and a rearrangement of the hydrogen associated with these bonds.[13] As a consequence, the Fermi energy may shift, depending on its position in the annealed state. As in our undoped samples, E_F is located near midgap, and there will be no significant shift of E_F. So changes in the properties of our junctions have to be interpreted in terms of a risen density of states in the vicinity of midgap.

Capacitance measurements offer relatively easy access to the $N(E)$ dependence. The results show an increase of more than one order of magnitude at 0.85 eV below E_c. This corresponds to the neutral dangling bond state in agreement with the interpretations of Kocka, Vanecek, and Schauer.[17]

Measurements of the photocurrent decay reflect an increase in charge density $n(E)$ after illumination. As noted above, $n(E)$ depends on the occupancy $f(E)$ of the states involved. $f(E)$ for its part depends on illumination and temperature. Thus $n(E)$ gives only a lower limit for the density of states $N(E)$. As the neutral dangling bonds do not emit

electrons into the conduction band within the measuring time (< 1 s) at room temperature, we cannot observe their contribution. That is why we attribute the rise in $n(E)$ to an increase in negatively charged dangling bonds. It is likely that at least part of these states are occupied under illumination and that they will take part in the emission processes during the transient.

The Staebler–Wronski effect reduces the photoconductivity[18] since the additionally created dangling bonds act as recombination centers. Nevertheless, we see no effect on the photocurrent of our samples. At a bias voltage of -5 V, the electric field across the a-Si:H layer amounts to about 5×10^4 V/cm. This leads to a *Schubweg* of the order of 100 μm. Compared to the thickness of the sample of 1 μm, the probability for recombination is negligible. Even a pronounced diminution of the *Schubweg* by the SWE has no influence on the photocurrent if it is greater than the a-Si:H thickness. Only in extreme cases of low fields that are found in the interior of the sample at zero bias is there recombination in our SBMIS diodes. This can be seen in the photocurrent-voltage characteristics (Fig. 3) where the photocurrent at zero bias reflects the influence of recombination on the short-circuit current by the Staebler–Wronski effect.

The behavior of SBMIS devices with respect to junction capacitance, steady state, and transient photocurrent can be understood on the basis of the normal Staebler–Wronski effect. But this effect does not predict the considerable rise in dark current observed. A possible explanation could be a reduction in the width of the barrier due to an increased density of states. The tunneling current through a-Si:H barriers is limited by thermionic field emission, as pointed out by Jackson *et al.*[19] Therefore, additional states should lead to a decrease of the effective barrier height and thus to an increase of I_d. But since the observed rise is not stable and disappears at room temperature with time constants in the order of hours, the explanation on the basis of the Staebler–Wronski effect can be ruled out.

Looking at Table I, several other possibilities can explain the barrier lowering observed. In our opinion, it is unlikely that new states are created at the interface by light soaking. Interface states are caused by the polarizability of the chemical bonds between semiconductor and metal or insulator, respectively. Although great efforts have been undertaken to reduce the interface-state density, a certain number of such states cannot be avoided. Therefore, these interface states are not expected to disappear quickly at room temperature.

Negatively charged bulk states could arise from trapping of photogenerated electrons in the space-charge region. However, they are inconsistent with the situation in our SBMIS junctions. From the relaxational behavior (Fig. 5) we conclude that the energetic depth of the states involved is between 1.0 and 1.4 eV. With reference to the barrier height of 0.86 eV,[8] these charged states would be below the Fermi energy. Therefore, an emission of electrons into the conduction band cannot take place.

Finally, we propose that interface states become positively charged, resulting in a barrier lowering. These states are located at the interface between the semiconductor and the insulator or inside the insulator, respectively. Their energetic position is 1.0–1.4 eV above the valence-band edge. Holes generated by prolonged illumination are trapped in these states. This leads to a barrier lowering as described above (see Table I).

Thermal excitation of trapped holes into the valence band can explain the barrier relaxation described above. However, we have to assume that holes can leave the interface states only thermally. The tunneling transitions from the hole traps to the metal or to the a-Si:H as well as recombination with electrons should be negligible.

A striking feature of the dark current increase is its dependence on the applied bias during light soaking. The degradation effect is strongly enhanced by a negative voltage at the ITO electrode. This reverse bias draws the photogenerated holes towards the a-Si:H/ITO interface and intensifies the trapping process. The Staebler–Wronski effect, on the contrary, is suppressed by a negative bias which prevents recombination within the a-Si:H layer.

One further observation points to the fact that interface states are responsible for the barrier degradation and relaxation: Samples measured under vacuum show a smaller effect than those investigated in air. Experiments with different ambients show a weak degradation and relaxation in dry ambients (N_2, O_2) and a strong effect in moist ambients (air, water vapor). So it is obvious that water is the most likely cause of the interface states mentioned above. We suggest that additional interface states are created by the presence of polar molecules, i.e., water. They change their charge state by trapping holes during prolonged illumination. This leads to the barrier lowering observed. From the slow relaxation process described above, we estimate their energetic position to be 1.0–1.4 eV above E_v.

The upper electrode of our diodes made from ITO has a porous structure.[20] Molecules can therefore diffuse to the interface and induce the formation of interface states. Once formed, these states remain even under vacuum. They can be annealed away at an elevated temperature. These ambient-induced defect states are still not fully understood and will be investigated more closely in the near future.

VI. CONCLUSIONS

In this paper, the influence of the creation and recharging of defect states in SBMIS diodes on the barrier height is investigated. An overview is given in Table II. The creation of bulk states (dangling bonds) by light soaking leads to

TABLE II. Effects of light-soaking and their origin.

Staebler–Wronski effect	Interface-state effect
Light soaking causes rise of bulk density of states	Light soaking causes barrier lowering by hole trapping
Forward current decreases	Reverse current increases
Transient photocurrent increases	Open-circuit voltage decreases
Junction capacitance increases	Short-circuit current decreases
Staebler–Wronski effect anneals above 200 °C	Barrier lowering recovers at room temperature

changes in transient photocurrents as well as in space-charge capacitance. The results are consistent with the normal Staebler–Wronski effect.

Water vapor diffusing through the ITO electrode towards the *a*-Si:H gives rise to interface states. They become positively charged after light soaking, which lowers the SBMIS barrier considerably. After resting the samples in the dark from several minutes up to a few days at room temperature, the barrier recovers. Hence we conclude that the interface states are about 1.0–1.4 eV above the valence-band edge.

ACKNOWLEDGMENTS

The authors would like to thank R. Primig, H. Doneyer, W. Müller, and E. Scheuermeyer for preparing the samples, and A. Kiendl for carrying out the CAD. The cross-sectional TEM pictures taken by S. Schild are gratefully acknowledged. We are indebted to A. Glade for stimulating discussions about the capacitance measurements and their interpretation, and to W. Fuhs for his helpful comments.

[1]K. Kempter, Proc. SPIE **617**, 120 (1986).
[2]M. Hoheisel, G. Brunst, and H. Wieczorek, J. Non-Cryst. Solids **90**, 243 (1987).
[3]W. Schottky, Z. Phys. **113**, 367 (1939).
[4]S. M. Sze, *Physics of Semiconductor Devices* (Wiley, New York, 1969), p. 363
[5]R. J. Nemanich, in *Semiconductors and Semimetals*, edited by J. I. Pankove (Academic, Orlando 1984), Vol. 21, p. 375.
[6]J. Bardeen, Phys. Rev. **71**, 717 (1947).
[7]K. Rosan and G. Brunst, MRS Symp. Proc. **70**, 683 (1986).
[8]M. Hoheisel, N. Brutscher, H. Oppolzer, and S. Schild, J. Non-Cryst. Solids **97&98**, 959 (1987).
[9]H. Wieczorek, thesis, Marburg, 1987.
[10]T. J. Mego, Rev. Sci. Instrum. **57**, 2798 (1986).
[11]A. Glade, thesis, Marburg, 1987.
[12]A. Glade, W. Fuhs, and H. Mell, J. Non-Cryst. Solids **59&60**, 269 (1983).
[13]M. Stutzmann, W. B. Jackson, and C. C. Tsai, Phys. Rev. B **32**, 23 (1985).
[14]H. Wieczorek and W. Fuhs, Phys. Status Solidi A **109**, 245 (1988).
[15]A. Glade, J. Beichler, and H. Mell, J. Non-Cryst. Solids **77&78**, 397 (1985).
[16]D. Jousse, R. Basset, S. Delionibus, and B. Bourdon, Appl. Phys. Lett. **37**, 208 (1980).
[17]J. Kocka, M. Vanecek, and F. Schauer, J. Non-Cryst. Solids **97&98**, 715 (1987).
[18]D. L. Staebler and C. R. Wronski, Appl. Phys. Lett. **31**, 292 (1977).
[19]W. B. Jackson, R. J. Nemanich, M. J. Thompson, and B. Wacker, Phys. Rev. B **33**, 6936 (1986).
[20]A. Mitwalsky, M. Hoheisel, W. Müller, and C. Mrotzek, Inst. Phys. Conf. Ser. **93**, 107 (1988).